Total Generalized Variation Based Joint Multi-Contrast, Parallel Imaging Reconstruction of Undersampled k-space Data

Adrian Martin[1,2], Itthi Chatnuntawech[1], Berkin Bilgic[3], Kawin Setsompop[3,4], Elfar Adalsteinsson[1,5], and Emanuele Schiavi[6]

[1]Department of Electrical Engineering and Computer Science, Massachusetts Institute of Technology, Cambridge, MA, United States, [2]Applied Mathematics, Universidad Rey Juan Carlos, Mostoles, Madrid, Spain, [3]A. A. Martinos Center for Biomedical Imaging, Department of Radiology, Massachusetts General hospital, Charlestown, MA, United States, [4]Harvard Medical School, Boston, MA, United States, [5]Harvard-MIT Health Sciences and Technology, Massachusetts Institute of Technology, Cambridge, MA, United States, [6]Universidad Rey Juan Carlos, Mostoles, Madrid, Spain

TARGET AUDIENCE: Researchers interested in undersampled multi-contrast imaging reconstruction combined with parallel imaging.

PURPOSE: Typical clinical MRI protocols include multiple acquisitions of the same region of interest under different contrast settings. Several methods that use the shared information across contrasts have been proposed to achieve better reconstruction of undersampled acquisitions compared to conventional reconstructions of each contrast in isolation[1,2,3]. The Total Generalized Variation (TGV) operator was recently introduced as a more flexible image prior than the Total Variation (TV) operator that has been typically used for applications such as denoising or parallel imaging reconstruction[4,5]. In this work, we extend the TGV operator to jointly reconstruct multiple MRI contrasts from undersampled k-space data using one or more receiver coils. The multi-contrast TGV operator (MC-TGV) exploits the structural similarities of the images. The proposed model achieves a better reconstruction accuracy measured in terms of Root Mean Squared Error (RMSE) compared to parallel imaging reconstruction methods like SENSE[6] and TV regularized SENSE (TV-SENSE)[7,8] (49.6% and 23.5% relative improvement for R=5 respectively).

METHODS: **Model proposed**. Let $u \in U$ be the multi-contrast complex image, with $U = \mathbb{C}^{MNL}$, where $M \times N$ are the number of rows and columns of the images, and L is the number of contrasts. We also define $V = \mathbb{C}^{MN2L}$, and $W = \mathbb{C}^{MN3L}$. We write the 2nd order MC-TGV as follows:

$TGV^2_{MC,\alpha}(u) = \min_{v\in V} \alpha|\nabla u - v|_{1V} + 2\alpha|\mathcal{E}(v)|_{1W}$, where $\mathcal{E}(v) = \frac{1}{2}(\nabla v + (\nabla v)^{T})$ is the symmetrized gradient and following Bredies[9] we define

$|p|_{1V} = \sum_{n=1}^{M\cdot N}\sqrt{\sum_{l=1}^{L}|p^l_{x,n}|^2 + |p^l_{y,n}|^2}$ and $|q|_{1W} = \sum_{n=1}^{M\cdot N}\sqrt{\sum_{l=1}^{L}|q^l_{x,n}|^2 + |q^l_{y,n}|^2 + 2|q^l_{xy,n}|^2}$. Let $k_{c,l}$ be the acquired Cartesian k-space data for coil c and contrast l, then we can formulate the Multi-Contrast Total Generalized Variation reconstruction (MC-TGV-SENSE) of undersampled images acquired with C coils as follows:

$$\min_{u\in U} TGV^2_{MC,\alpha}(u) + \sum_{c=1}^{C}\sum_{l=1}^{L}\left\|\Omega_l \mathcal{F} S_c u - k_{c,l}\right\|_2^2.$$

Here S_c denotes the cth coil sensitivity profile, $\mathcal{F}$ the Fourier transform and Ω_l the undersampling mask for the l^{th} contrast. We solve this minimization problem by applying a primal-dual algorithm[10]. For this purpose, the minimization problem is transformed into the equivalent saddle-point problem using duality arguments on the MC-TGV operator[9]. **Validation.** We compared the performance of the proposed model to SENSE and TV-SENSE, both implemented using a non-linear conjugate gradient method[11]. Three different contrasts and 23 slices were acquired fully sampled from a healthy volunteer at 3T using turbo spin-echo at 0.9x0.9x3 mm^3 resolution with FOV = 22cm x 22cm, TEs = 22/55/99ms, and TR = 4s. The 32-channel data were first combined and reconstructed. The corresponding k-space data were then retrospectively undersampled along the phase encoding direction with an acceleration factor of four, five and six (R = 4, 5, 6) in MATLAB and projected using 8 simulated sensitivity coil profiles[12]. For each method, we selected the undersampling type (uniform vs random) that minimizes RMSE. Different undersampling patterns were used for each contrast.

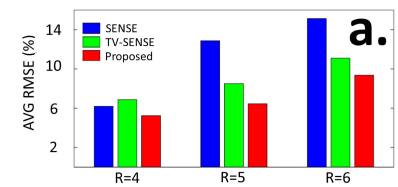

RESULTS: Figure **a.** shows the averaged RMSE (AVG. RMSE) across the three reconstructed contrasts at different R. The proposed method outperforms SENSE (TV-SENSE) with a relative improvement of 15.5% (23.9%), 49.6% (23.5%) and 38.2% (15.7%) for R=4, 5 and 6, respectively. Figure **b.** shows representative results of these 3 algorithms at R=5. MC-TGV-SENSE achieves the best RMSE for the three contrasts. The sum of the absolute differences (SAD) across the three images is displayed in the last column. Both SENSE and TV-SENSE difference maps show more severe structural errors when compared with the proposed method. This can also be appreciated in the detail of the reconstructed slice of the first echo shown in Figure **c.** Undersampling artifacts are clearly visible in SENSE and to a lesser extent in TV-SENSE reconstruction. The MC-TGV operator eliminates the artifacts and avoids the staircase artifact that is inherent in TV-based reconstructions.

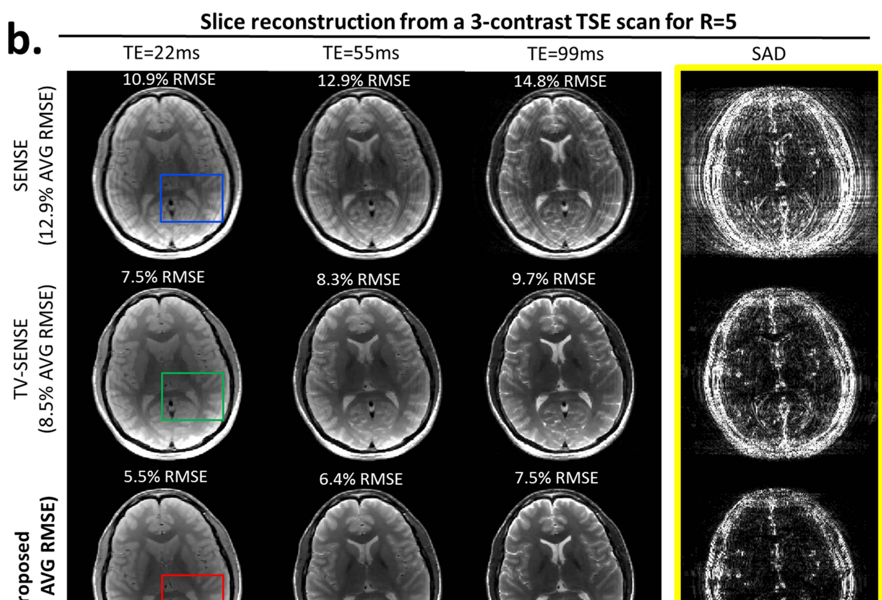

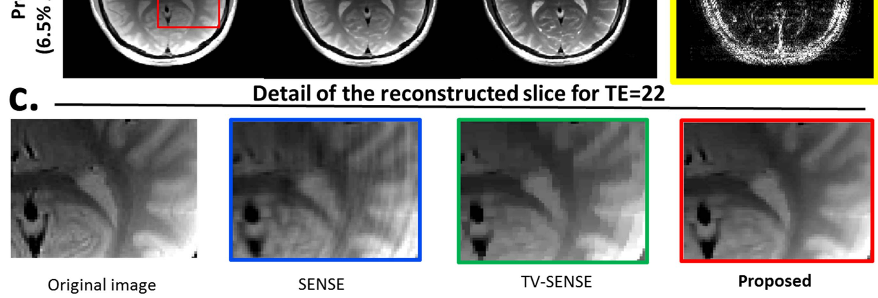

DISCUSSION: The proposed multi-contrast TGV operator allows information sharing across contrasts while better preserving idiosyncratic details in each image by promoting piecewise linear discontinuous solutions. Coupled with the encoding power of receive arrays, it yields improved data quality relative to SENSE and TV-SENSE solutions. Further work includes the application of the proposed technique to MR Fingerprinting where highly undersampled data with multiple coils are acquired for many different contrast settings[13].

ACKNOWLEDGMENTS: Project TEC2012-39095-C03-02 of the Spanish Ministry of Economy and Competitiveness. R01 EB017219, EB006847, EB017337.

REFERENCES: [1] Bilgic B. et al. MRM (2011); [2] Huang J. et al. MICCAI (2012); [3] Majumdar A. et al. MRM (2011); [4] Knoll F. et al MRM (2011); [5] Knoll F. et al MRM (2012); [6] Pruessman KP. et al MRM (2001) [7] Liu B. et al MRM (2009); [8] Otazo R. et al MRM (2010) [9] Bredies K. LNCS (2014); [10] Chambolle A. et al J M Imaging Vis (2011); [11] Lustig M. et al MRM (2007); [12] Lin, F H. et al Hum. Brain Mapp (2003); [13] Ma D. et al Nature (2013).